EFFECTS OF INTERNAL HYDROGEN ON FRACTURE BEHAVIOUR OF A508.3 STEEL AT LOW TEMPERATURES

J.Sojka*, J.Galland†, L.Hyspecka**, M.Tvrdy*

The effect of internal hydrogen is studied on the fracture behaviour of A508.3 steel in the temperature range from +20 to -196°C. The main manifestation of the increased hydrogen content in the steel is the presence of fish eyes on fracture surfaces nucleating on coarser globular oxi-sulphidic inclusions. Quantitative fractographic analysis of fish eyes showed the significant changes of their geometric parameters with the temperature. These changes are explained by means of Pressouyre's concept of residual and applied stresses in the presence of hydrogen.

INTRODUCTION

Low alloy Mn-Ni-Mo steel A508.3 used in nuclear power engineering especially as a pressure vessel steel is subject of a large research for more than 25 years. Apart from detailed studies of mechanical properties of this steel in "inert" conditions including the local approach method a considerable attention was paid also to the study of its susceptibility to stress corrosion cracking, corrosion fatigue and hydrogen embrittlement. The results obtained show relatively high susceptibility of A508.3 steel to hydrogen embrittlement, which in macroscopic scale results mainly in ductility losses. Direct observation of hydrogen-dislocation interactions by means of electron microscopy has shown that hydrogen enhanced localised plasticity comes into play in this steel.

This paper deals with the study of the effects of internal hydrogen on fracture characteristics of A508.3 steel after conventional heat treatment and especially with the quantitative fractographic analysis of fish eyes which were found on fracture surfaces. This evaluation was performed in the temperature range from +20 to -196°C with use of tensile tests.

* Research Institute of Vitkovice, Czech Republic
† Laboratory C.F.H., Ecole Centrale Paris, France
** Technical University Ostrava, Czech Republic

EXPERIMENT

A heavy forging of A508.3 steel with the wall thickness approx. 200 mm was used for experimental studies. The steel was produced with the addition of CaSi in order to reduce the sulphur content and to modify the shape of sulphidic inclusions. The chemical composition of the investigated steel is given in Table 1.

TABLE 1 - Chemical composition (% by mass)

C	Mn	Si	P	S	Cu	Ni	Cr	Mo
0,21	1,35	0,20	0,008	0,003	0,006	0,78	0,13	0,50

Steel was used after conventional heat treatment comprising normalising 880°C/6h/air, quenching 860°C/3h/water and tempering 640°C/7h/air. The tensile tests were realized with use of smooth cylindrical specimens with 4 mm gage diameter at the temperatures of +20, -10, -60, -100 and -196°C and at the deformation rate $\dot{\varepsilon}=6.10^{-5}s^{-1}$. Initial state was evaluated as well as the state after cathodic charging. This charging was carried out at room temperature in the water solution of hydrochloric acid with the addition of potassium rhodanide and hydrazine for 24 hours at the current density $5mA/cm^2$. Metallographic analysis was performed by the methods of optical and scanning electron microscopy, including the methods of image analysis and local chemical analysis.

RESULTS AND DISCUSSION

It was ascertained by high temperature analysis of the hydrogen content that the steel contained in the initial state approx. 0,9 ppm of hydrogen and after cathodic charging it contained about 8 ppm of hydrogen. The steel microstructure corresponded mostly to tempered granular bainite, in segregation bands to tempered lower bainite. The dependence of principal mechanical properties of A508.3 steel on the testing temperature for both evaluated states, i.e. the initial state and the state after hydrogen charging, is shown in Figure 1. It turns out that the yield strength and the ultimate tensile strength values were influenced only negligibly by increased hydrogen content in the steel. The drop of plastic properties, expressed here by the reduction of area, was on the contrary very pronounced in the whole studied temperature range, with the exception of the temperature -196°C where hydrogen embrittlement did not appear due to strongly limited hydrogen diffusivity. A qualitative fractographic analysis has shown that the failure mode in initial state has remained transgranular ductile to the temperature of -100°C. At -196°C a transgranular cleavage fracture was observed which was identical for both evaluated states. The presence of the increased hydrogen content in steel has manifested itself on fracture surfaces of specimens tested between +20 and -100°C mainly by the presence of fish eyes (Fig.2). The size of fish eyes was getting smaller with the decreasing temperature. The dimension of the biggest ones exceeded 1 mm at the temperature +20°C. The fish eyes were distributed on fracture surfaces very heterogeneously, the remaining part of the fracture surface - depending on the testing temperature - being either mostly transgranular ductile or transgranular cleavage.

Due to a considerable role of non-metallic inclusions in this case a chemical composition of inclusions was determined on metallographic sections and on

fracture surfaces. The inclusion content in the steel was then determined by image analysis method. The non-metallic inclusions analysed on metallographic sections were identified in most cases as complex oxides containing to variable quantities namely Al, Mg, Si and Ca, the outer shell being formed by (Ca,Mn)S. Individual, slightly elongated pure manganese sulphides were observed only to a small extent. Analysis of the chemical composition of non-metallic inclusions on the fracture surfaces in the centres of fish eyes has shown that the fish eyes were formed in principle around all types of non-metallic inclusions with the exception of manganese sulphides. Nucleation of defects occurred primarily by separation of the inclusion-matrix interface (Fig.3). When measured the non-metallic inclusion content in the steel by means of the image analysis method only basic parameters were evaluated, i.e. area fraction of inclusions A_A, number of inclusions per unit area N_A, mean diameter of inclusions d and Feret diameters d_x and d_y. The results which are given in Table 2 show that the inclusion content in steel is very low. Detailed analysis has proved, however, that non-metallic inclusions were distributed very heterogeneously in the matrix.

TABLE 2 - Results of quantitative analysis of non-metallic inclusion content

A_A(%)	N_A(mm^{-2})	d(μm)	d_x(μm)	d_y(μm)	d_x/d_y
0,018±0,007	7,3±1,3	4,3±0,5	4,8±0,6	4,7±0,7	1,02±0,06

Analysing the literature data it is possible to define those parameters of non-metallic inclusions, which play the decisive role at the defect formation in the presence of hydrogen. These are mainly: Type of inclusions, their shape, size and their content in steel(1). Speaking of the type of non-metallic inclusions a criterion of utmost importance for evaluation of possible hydrogen effects is a value of interaction energy hydrogen - non-metallic inclusion. Data about hydrogen interaction energy for individual types of inclusions are not, however, homogeneous in the literature and for complex oxi-sulphides in steels produced with CaSi addition are still missing. Elongated elliptic inclusions are considered to be the most detrimental. Coarser inclusions are generally considered to be more detrimental than the smaller ones due to the fact that hydrogen concentration in the local volume surrounding the inclusion is here higher. As to the content of non-metallic inclusions, it was ascertained in many cases that a critical content of inclusions exists when the hydrogen effect is the most significant.

The fish eyes represents the defects which are always connected with the higher hydrogen content in steels and are more typical for castings and weld metal. They are observed also in heavy forgings. From the point of view of fish eye formation manganese sulphides are considered to be the most dangerous type, especially when they are elongated. Nevertheless, recent works devoted to the problems of fish eyes show that in case of steel produced with the addition of CaSi namely the coarser globular oxi-sulphides provoke the fish eye formation and not the manganese sulphides, although they are also present in the steel. It seems that the decisive criterion is here rather the size of inclusions than their type(2). These findings correspond also with results of our observations. In the case we studied the presence of fish eyes in steel after hydrogen charging can be explained mainly by the low content of non-metallic inclusions, which are however rather coarse and not homogeneously distributed in the matrix.

Owing to the fact that qualitative fractographic analysis has shown that both the number and the size of fish eyes changed considerably with the testing temperature, a quantitative analysis of geometric parameters of fish eyes was realized. The following parameters were measured: d_i - mean diameter of the fish eye and d_{oi} - mean diameter of the non-metallic inclusion in its centre. Number of fish eyes per unit area N_A was subsequently calculated. The main results of the quantitative analysis are summarised in Figures 4 and 5. At all studied temperatures it is obvious that the coarser the non-metallic inclusion, the bigger fish eye it causes (Fig.4). It hence follows from the results represented in Fig. 5, in spite of high scatter of experimental results, that the decrease in testing temperature results in reduction of sizes of both the fish eyes and the non-metallic inclusions in their centres, while the number of fish eyes per unit area increases. These changes can be explained if we take into consideration Pressouyre's concept of residual σ_r^H and applied σ_a^H stresses in the presence of hydrogen, the necessary condition for the defect nucleation being the fact that the sum of all the residual and applied stresses σ_{tot}^H exceeds the local cohesive strength σ_c^H.

The applied stress is given namely by the yield strength as it is presumed that fish eyes are formed during external loading in the region of the plastic deformation. On the other hand, the residual stress depends on the local hydrogen concentration, i.e. it increases with growing size of non-metallic inclusions. At higher temperature, when the yield strength is considerably lower, a higher residual stresses are necessary for the crack nucleation. These stresses are attained only around large inclusions. On the contrary, at lower temperature, when the yield strength is higher, lower residual stresses and therefore smaller inclusions are sufficient to exceed the local cohesive force and to form the cracks. Changes in the fish eye size with the testing temperature can be in the first approximation associated with the critical defect size which decreases with the decreasing temperature.

CONCLUSIONS

The study of hydrogen effects on the fracture behaviour of A508.3 steel at low temperatures has shown that the main manifestation of the increased hydrogen content in the steel was the presence of fish eyes on fracture surfaces. Nucleation of the fish eyes occurred on the coarser, but globular oxi-sulphides and not on the smaller, although elongated manganese sulphides. By means of the quantitative fractography in was ascertained that with the decreasing temperature the size of fish eyes decreased as well as the size of inclusions on which the fish eyes had nucleated, while the number of fish eyes increased. It was possible to explain these changes by different level of residual and applied stresses for different testing temperatures in the sense of Pressouyre's concept.

REFERENCES

(1) Pressouyre, G.M. et al, Mém. et Etudes Scientifiques, Vol. 79, 1982, pp. 161-176, 217-228.

(2) Maurer, K.L. et al, Hutnik, 1989, No. 7-8, pp. 256-262.

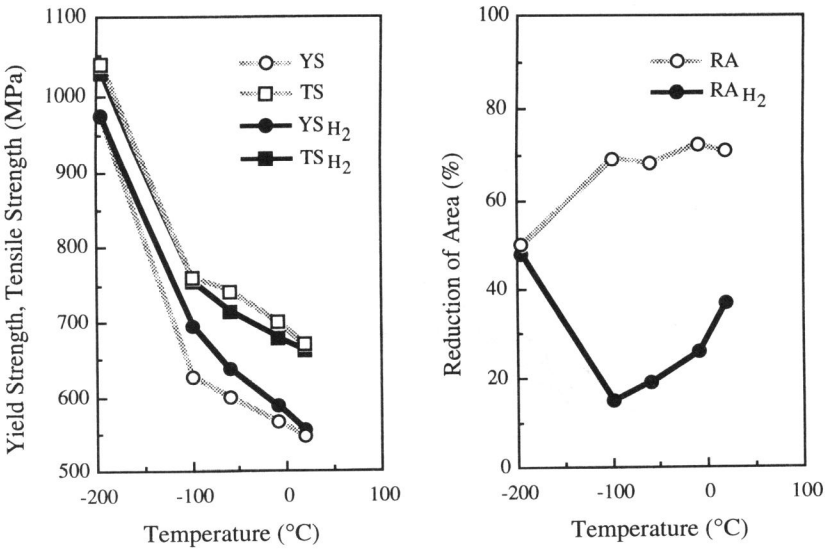

Figure 1 Dependence of yield strength (YS), tensile strength (TS) and reduction of area (RA) on the testing temperature for the both studied states

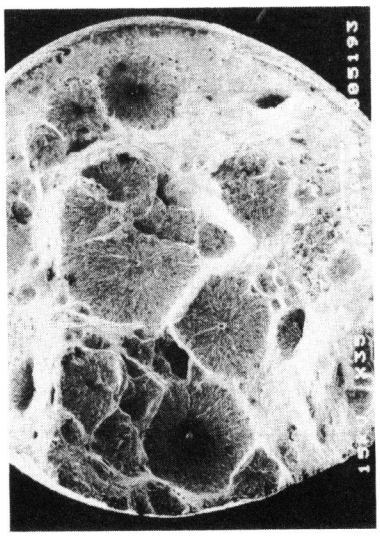

Figure 2 Fish eyes on the fracture surface (test. temperature -60°C)

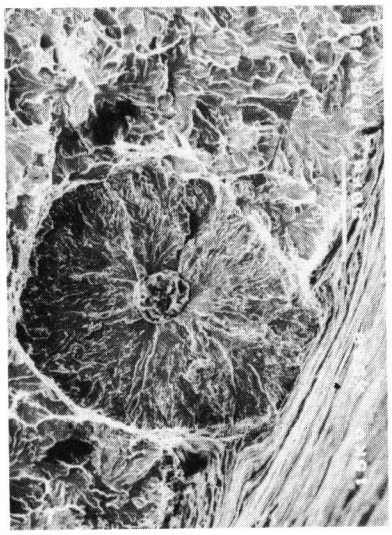

Figure 3 Globular inclusion in the centre of the fish eye

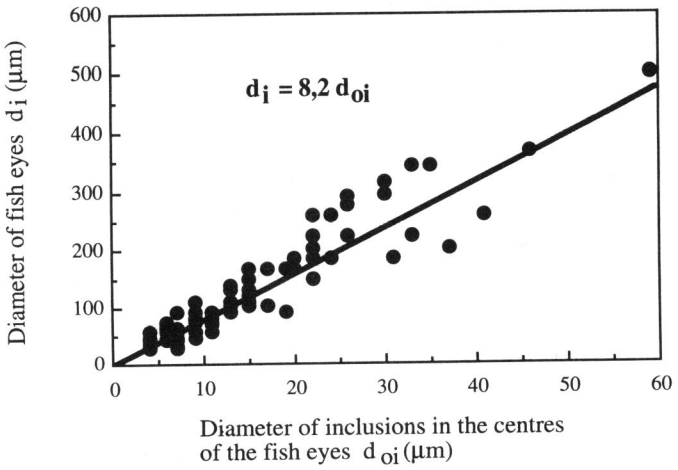

Figure 4 Dependence of the fish eye diameters on the diameters of inclusions in their centres (testing temperature -100°C)

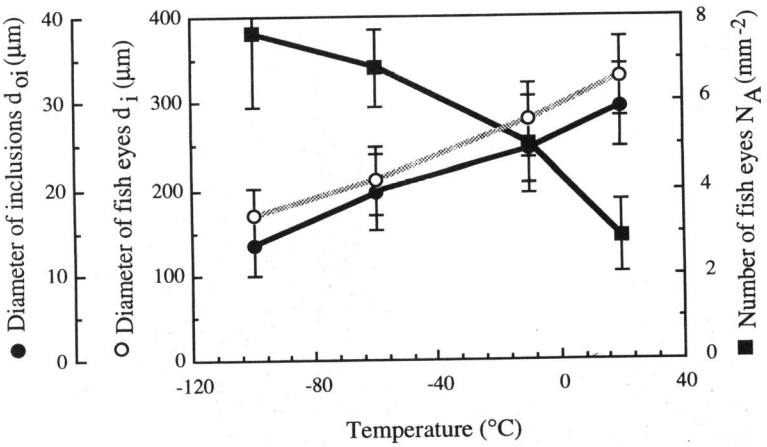

Figure 5 Influence of testing temperature on geometric parameters of fish eyes